



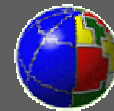
XCIX CONGRESSO NAZIONALE

Relazione Generale Sezione IVa

# PHYSICAL PROCESSES OCCURRING DURING AN EARTHQUAKE: WHAT CAN WE LEARN FROM MODELS OF SEISMIC SOURCES?

Andrea Bizzarri

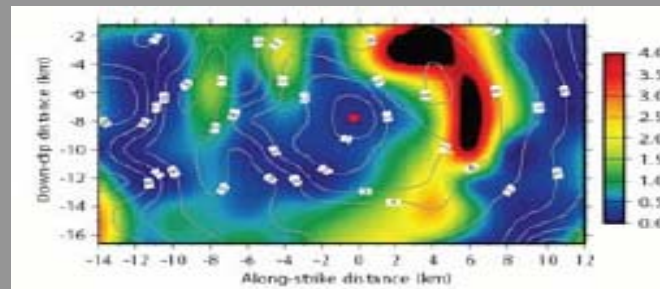
Istituto Nazionale di Geofisica e Vulcanologia – Sezione di Bologna



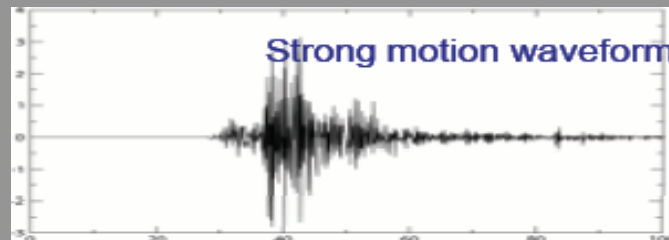
*25 Settembre 2013*

# Seismologists need traction

- ✓ To apply fracture mechanics on mathematical planes representing the fault surfaces;
- ✓ To numerically simulate the spontaneous rupture nucleation, propagation, healing and arrest in dynamic earthquake models;



- ✓ To model seismic wave propagation in the surrounding medium;



- ✓ To predict ground shaking.



# Stochastic or deterministic?

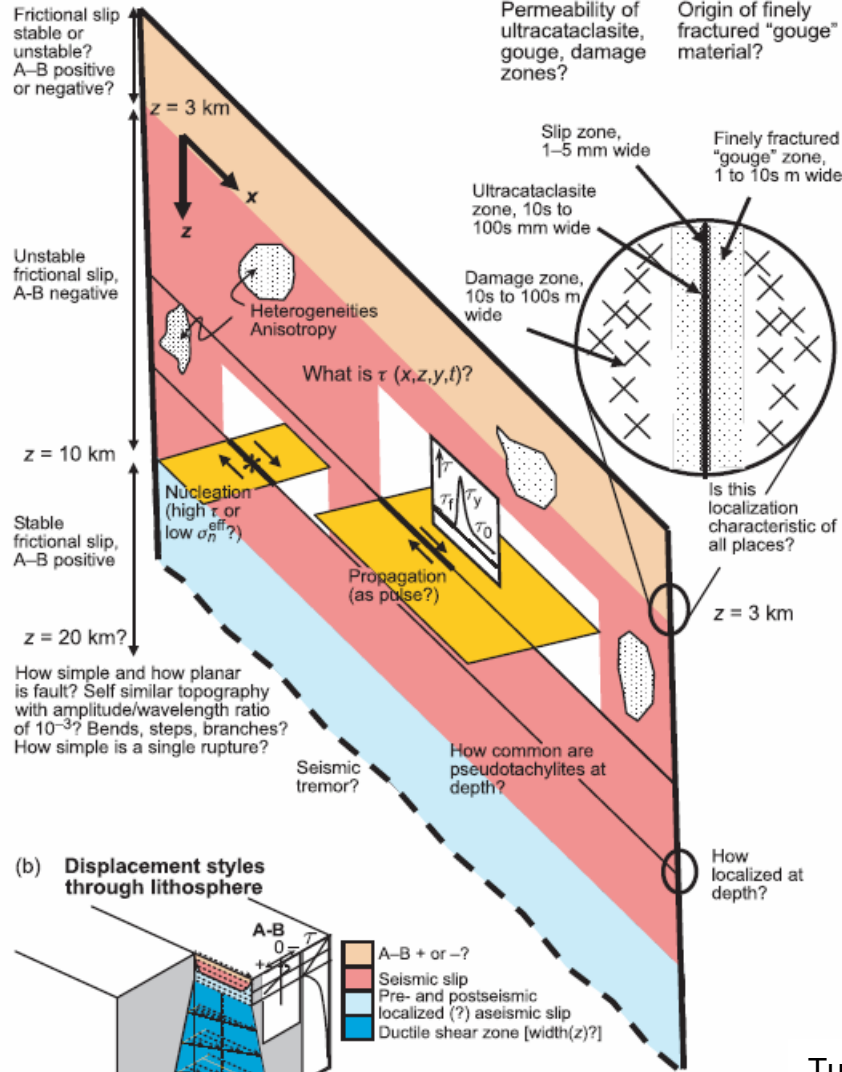
- ✓ **Stochastic** (or statistic) models: several aspects of the phenomenon under study are out of range, and they are replaced by unknowable, and hence random, processes, whose behavior cannot be predicted exactly but can be described in probability terms:
  - Gutenberg–Richter law
  - Omori law
- ✓ **Deterministic** (or physical) models: aim to understanding (and hence to predict) all the details of the considered phenomenon which does not include random components.

# Central issues

- ✓ Quantitative ( instrumental ) seismology is a relatively juvenile discipline
- ✓ Contrary to other fields of science, we can not plan natural ( i.e., at real–world scale ) experiments ( like biology, chemistry, etc. )...
- ✓ ... and we do know the PHYSICS, i.e., what are the exact equations which completely describe the complex fault systems ( on the contrary, climatologists, e.g., know the equations to be solved through numerical experiments )...
- ✓ ... and we do not know the initial conditions.

# Fault models

## (a) Seismogenic part of fault



Tullis et al. (2007, MIT Press)

What are temporal and spatial distributions of displacement at transitions within and beneath lithosphere?

## Internal Structure of Principal Faults of the North Branch San Gabriel Fault

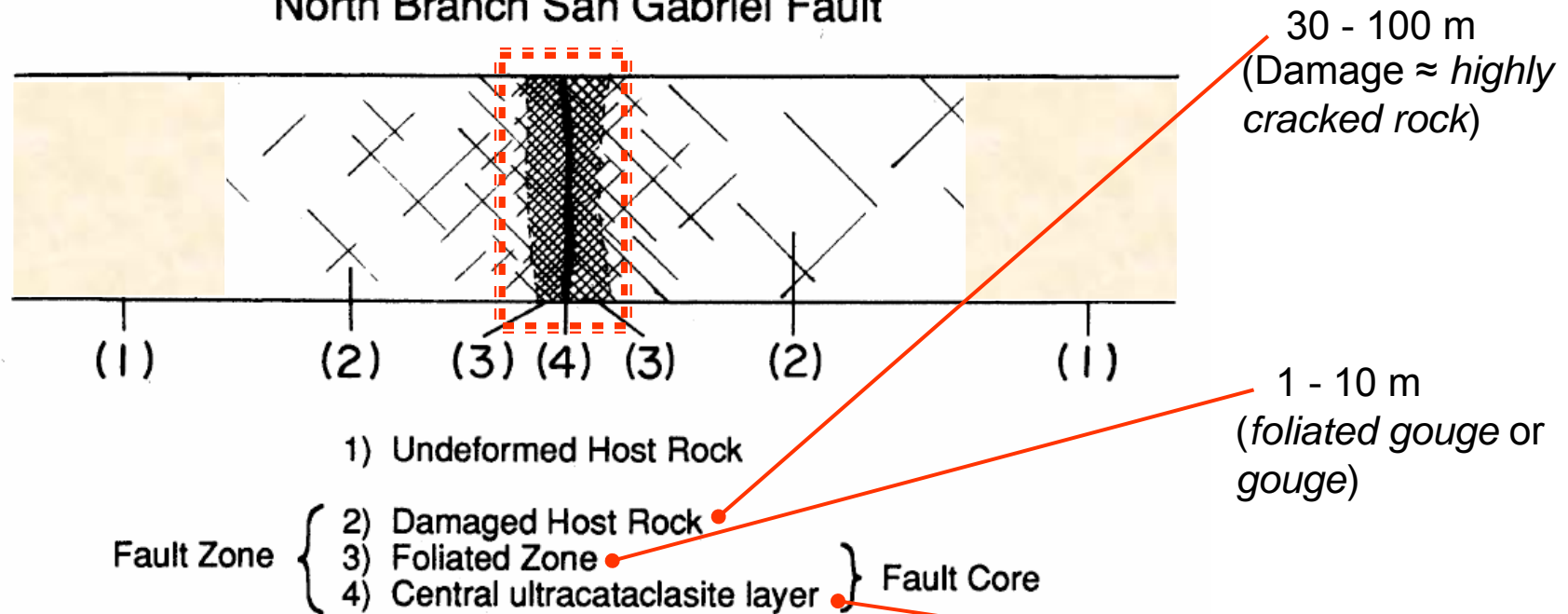
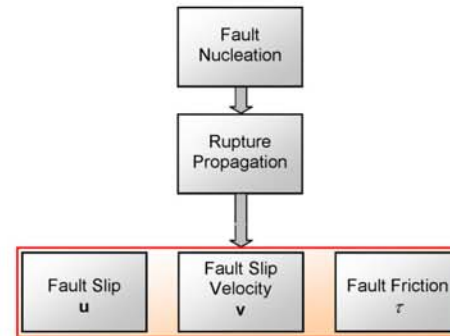


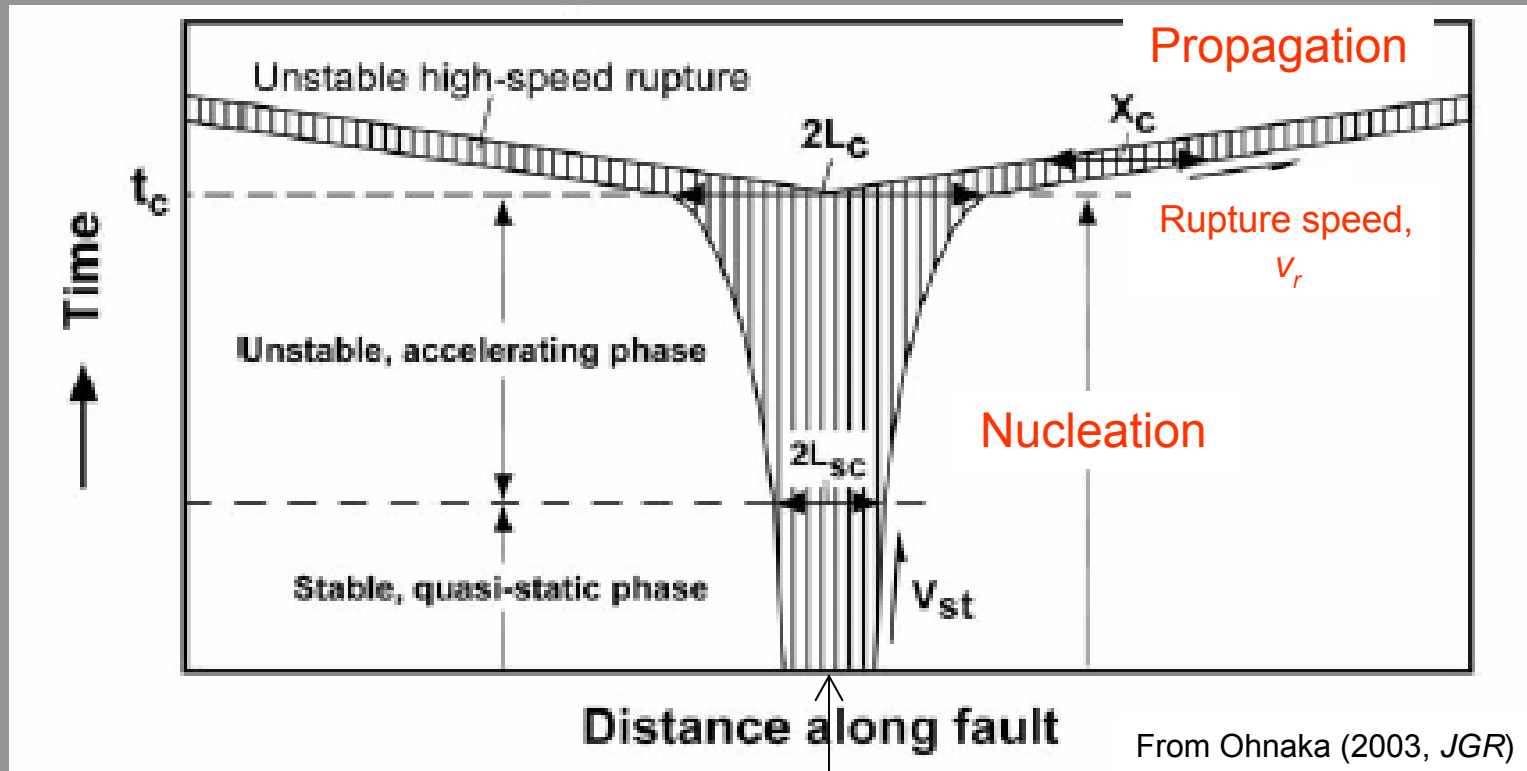
**Fig. 2. Schematic section across the North Branch San Gabriel fault zone illustrating position of the structural zones of the fault. The diagram is not to scale.**

Chester et al. (1993, *J. Geoph. Res.*)  
 Sibson (2003, *BSSA*)  
 Chester and Chester (2004, *SSA, SCEC meetings*)

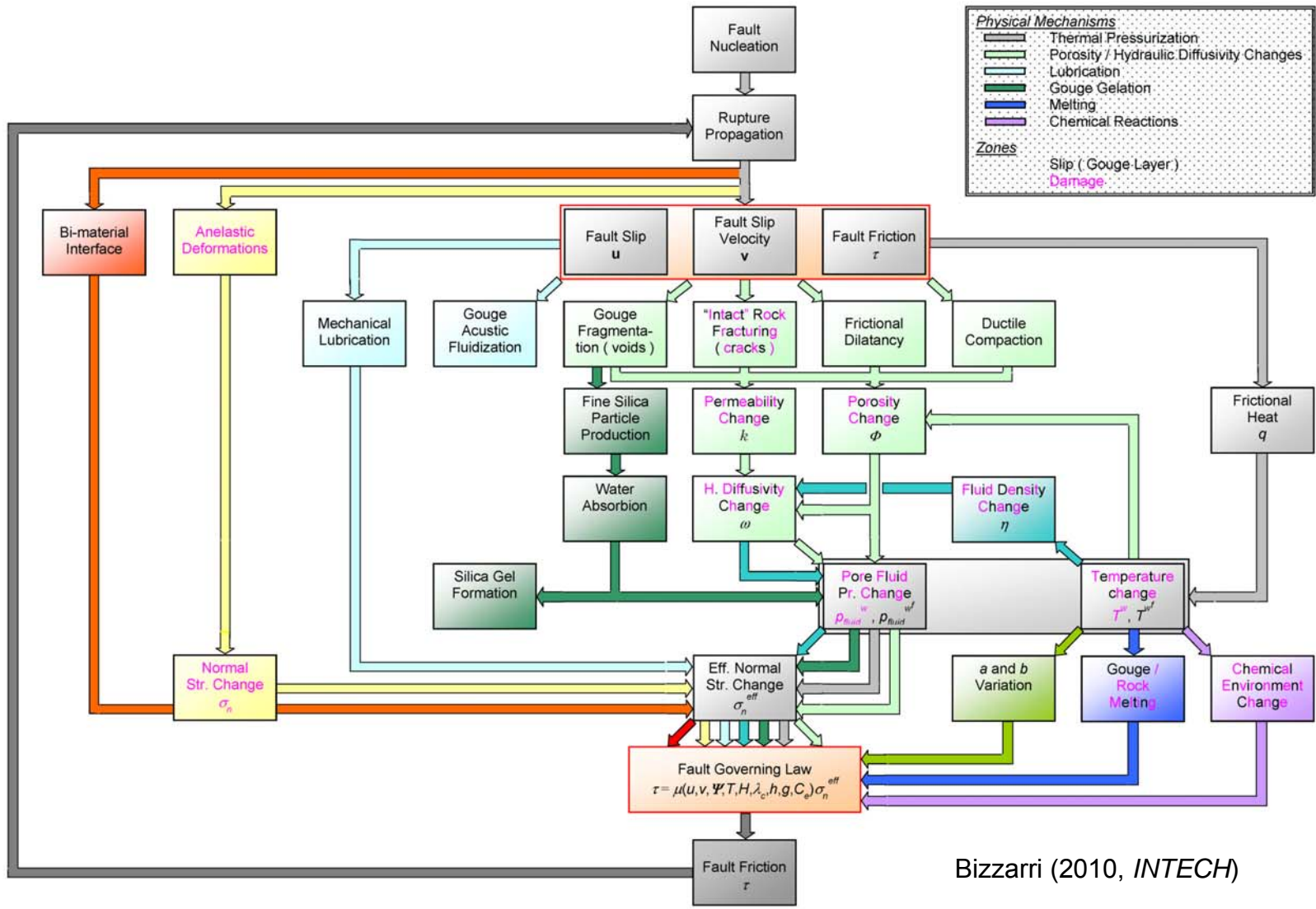
# Physical Phenomena in Faulting



# Sketch of an expanding bilateral rupture







Bizzarri (2010, INTECH)

# Fracture Criteria & Constitutive Laws

- In full of generality we can express the constitutive ( or governing ) as:

$$\tau = \mu(u, v, \Psi, T, H, \lambda_c, h, g, C_e) \sigma_n^{eff}(\sigma_n, p_f)$$



where:

1st – order dependencies

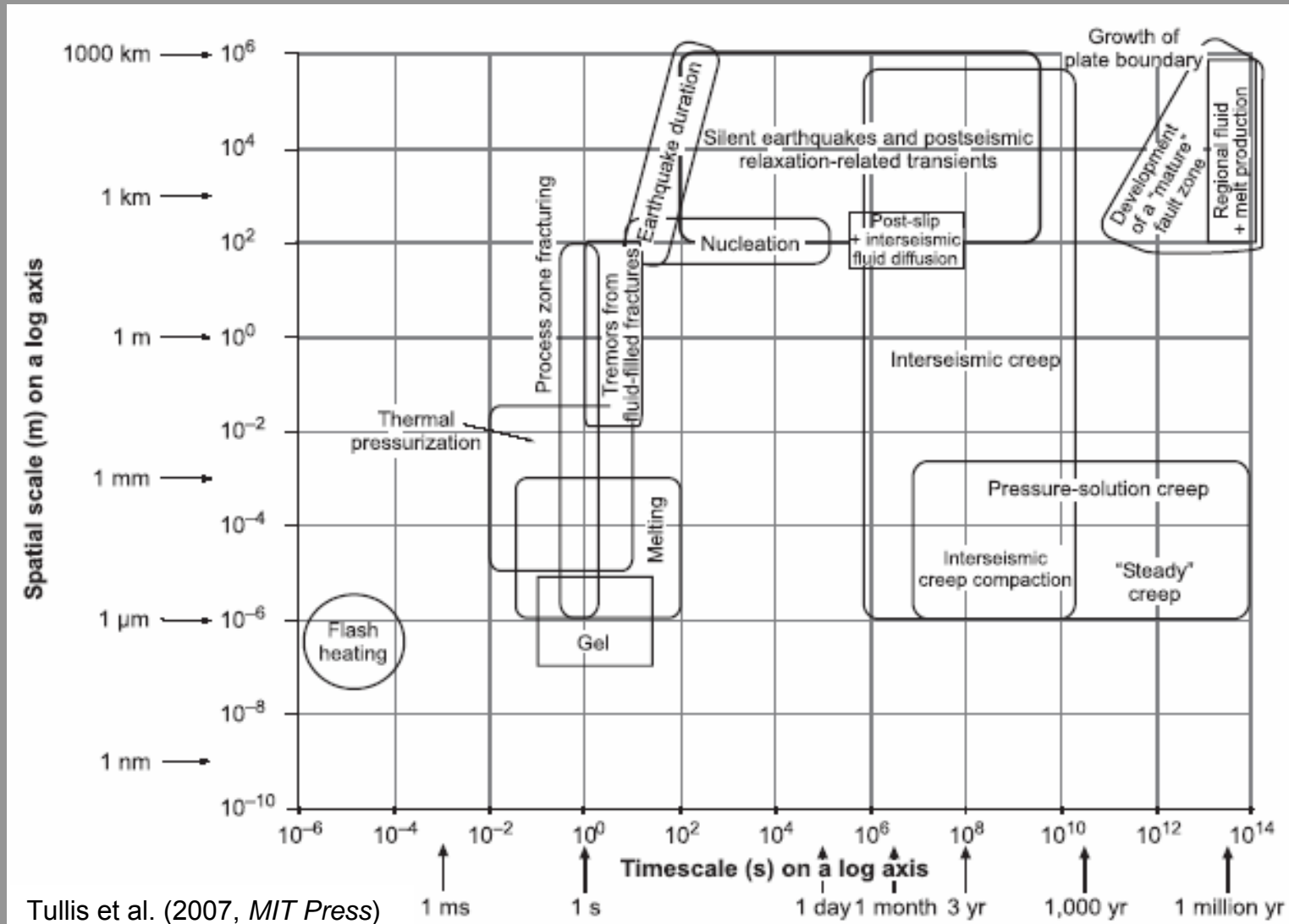
- $u$  is the slip ( i. e. displ. disc. ) modulus, ←
- $v$  is the slip velocity modulus ( its time der. ), ←
- $\Psi = ( \Psi_1, \dots, \Psi_N )$  is the state variable vector, ←
- $T$  is the temperature ( related to ductility, plastic flow, melting and vaporization ),
- $H$  is the humidity,
- $\lambda_c$  is the characteristic length of surface ( accounting for roughness and topography of asperity contacts ),
- $h$  is the hardness,
- $g$  is the gouge ( accounting for surface consumption and gouge formation ),
- $C_e$  is the chemical environment

# Occam's razor

- ✓ We follow the logical principle of simplicity ( i.e., the Occam's razor ):

The simplest way to describe the fault complexity is to **start from the beginning** ( i.e., from the canonical formulations of the governing equations ) and then **add** to the model **one by one** all additional phenomena until the empirical ( instrumentally recorded ) evidence can be explained.

# Spatial and temporal scales



# Towards real – world conditions

$u_{tot} \sim$  several m

$v \sim$  several m/s

$\sigma_n^{eff} = 100 - 200$  MPa

Classical laboratory

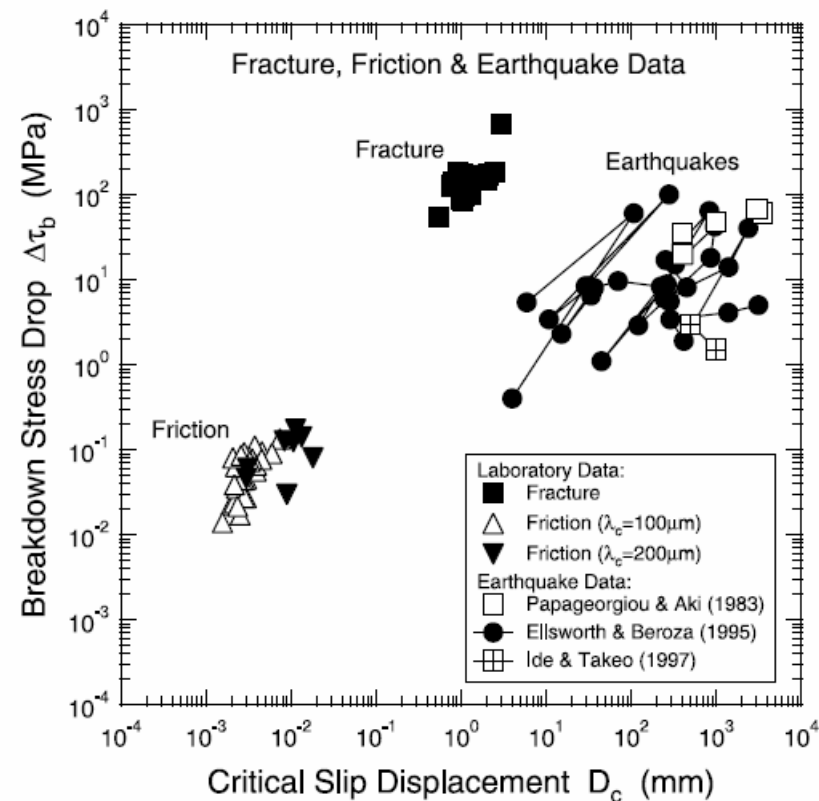
stick – slip experiments

( Dieterich, 1981 )

$u_{tot}$  up to 1.4 mm

$v$  up to  $25 \mu\text{m/s}$

$\sigma_n^{eff} = 10$  MPa



From Ohnaka (2003)

## High velocity rotary friction apparatus



$U_{tot} = \text{infinite}$

$v = 0.1 \mu\text{m/s} - 10 \text{ m/s}$

$\sigma_n^{eff} < 20 \text{ MPa}$

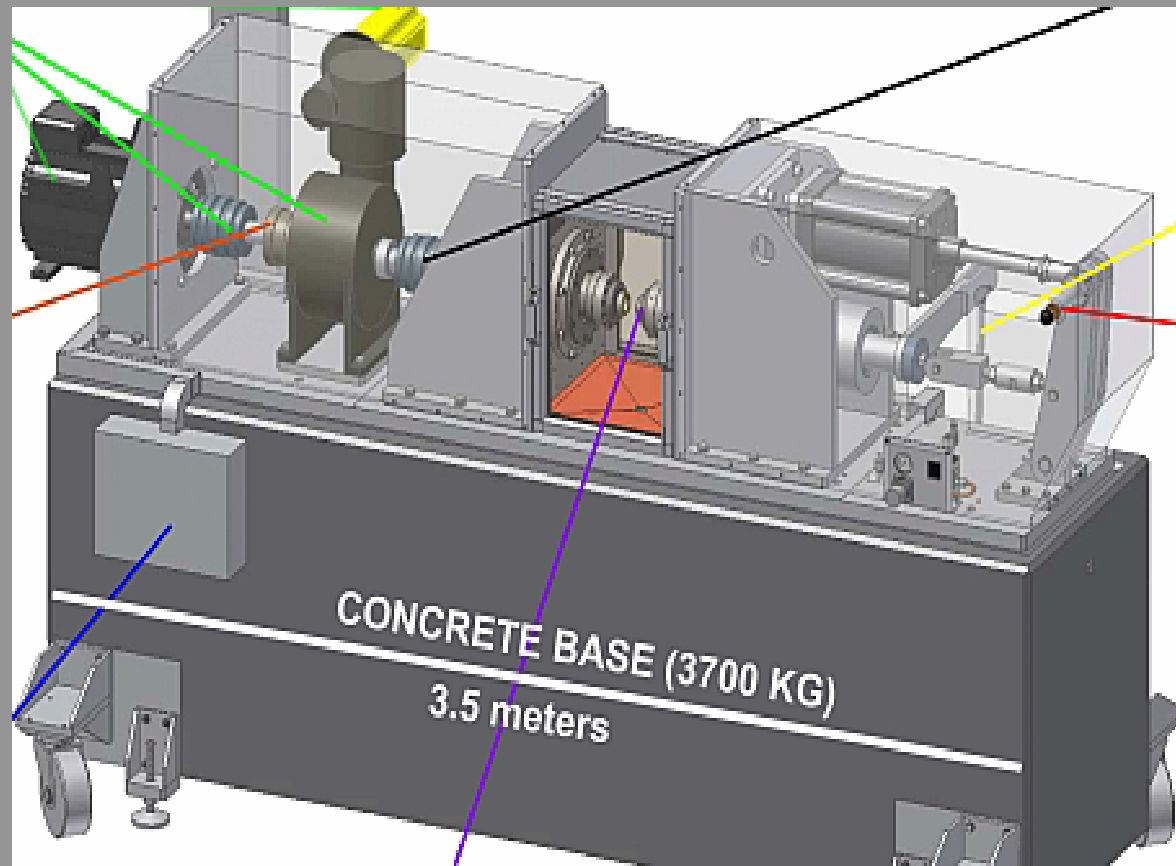
Shimamoto and Tsutumi (2004,  
*Str. Geol.*)

# High velocity rotary friction apparatus @ INGV

$u_{tot} = \text{infinite}$

$v = 1 \mu\text{m/s} - 9 \text{ m/s}$

$\sigma_n^{eff} < 70 \text{ MPa}$



Niemeijer et al. (2009, AGU Fall Meeting)

# Statement of the problem and methodology



We solve *fully dynamic, spontaneous problem* ( the fundamental elasto–dynamic equation ), without body forces  $\mathbf{f}$

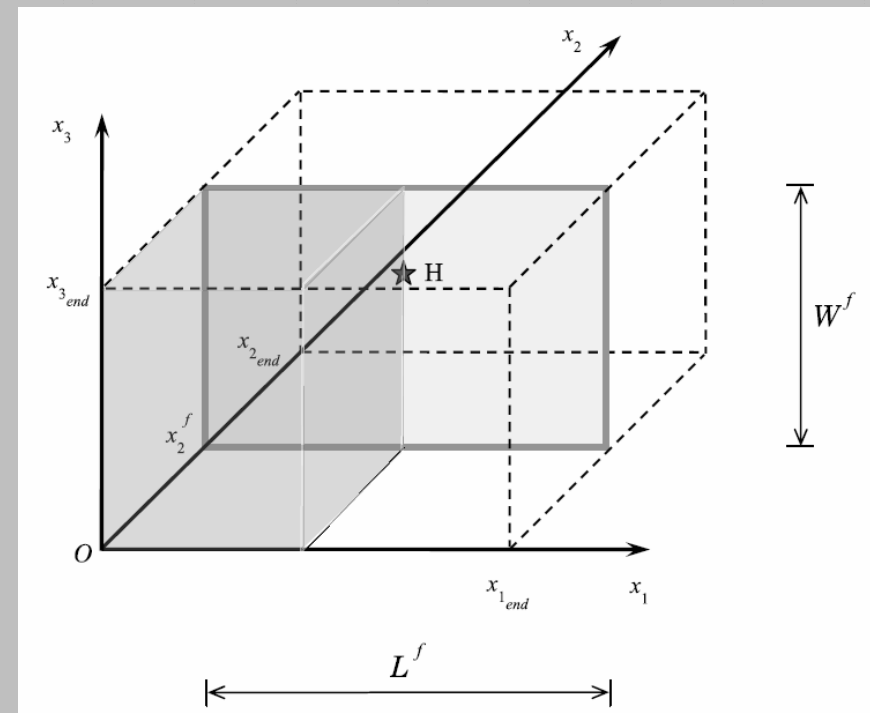
$$\rho \ddot{U}_i = \sigma_{ij,j} + \cancel{f_i}$$

We consider a *truly 3–D problem*, for which the solutions are in the form  $\mathbf{u} = (u_1(x_1, x_3, t), 0, u_3(x_1, x_3, t))$ , and so on

The fault plane  $\Sigma$  can be governed by *different constitutive laws*

The solution of the elasto–dynamic problem is obtained numerically, by using *2<sup>nd</sup>–order accurate, finite–difference code*

Bizzarri and Cocco (2005, *Ann. Geophys.*); Bizzarri and Spudich (2008, *JGR*)

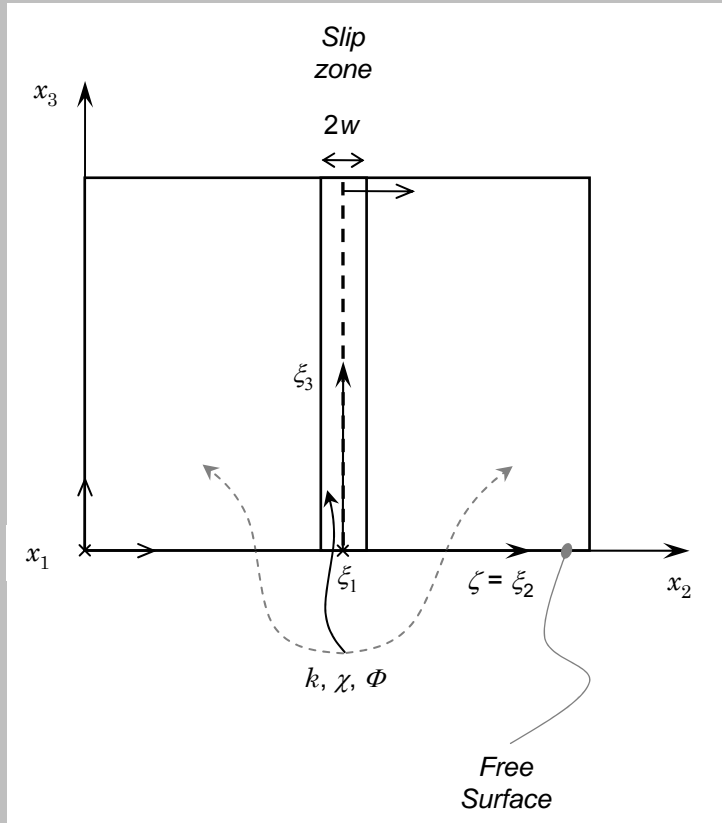




An aerial photograph of a coastal wetland or marsh. The landscape is a mix of light-colored, sandy or silty areas and darker, more vegetated or water-saturated regions. The terrain appears flat with some subtle depressions and channels. A semi-transparent grey rectangular box is centered over the image, containing the text "I. Thermal pressurization of pore fluids" in a bold, red, sans-serif font.

**I. Thermal pressurization  
of pore fluids**

# Mathematical background



1 - D Fourier' s heat conduction equation:

$$\frac{\partial}{\partial t} T = \chi \frac{\partial^2}{\partial \zeta^2} T + \frac{1}{c} q$$

Coupling of temperature  $T$  with pore fluid pressure  $p_{fluid}$ :

$$\frac{\partial}{\partial t} p_{fluid} = \frac{\alpha_{fluid}}{\beta_{fluid}} \frac{\partial}{\partial t} T - \frac{1}{\beta_{fluid} \Phi} \frac{\partial}{\partial t} \Phi + \omega \frac{\partial^2}{\partial \zeta^2} p_{fluid}$$

where  $\chi$  is the thermal diffusivity,  $c$  the heat capacity for unit volume,  $\alpha_{fluid}$  the coefficient of thermal expansion,  $\beta_{fluid}$  the compressibility coefficient,  $\Phi$  the porosity and  $\omega = k/\eta_{fluid}\beta_{fluid}\Phi$  the hydraulic diffusivity (being  $k$  the permeability of the medium and  $\eta_{fluid}$  the dynamic fluid viscosity). Analytical solutions at  $\zeta = 0$  are:

$$T^{wf}(\xi_1, \xi_3, t) = T_0^f + \frac{1}{2cw(\xi_1, \xi_3)} \int_0^{t-\varepsilon} dt' \operatorname{erf}\left(\frac{w(\xi_1, \xi_3)}{2\sqrt{\chi(t-t')}}\right) \tau(\xi_1, \xi_3, t') v(\xi_1, \xi_3, t')$$

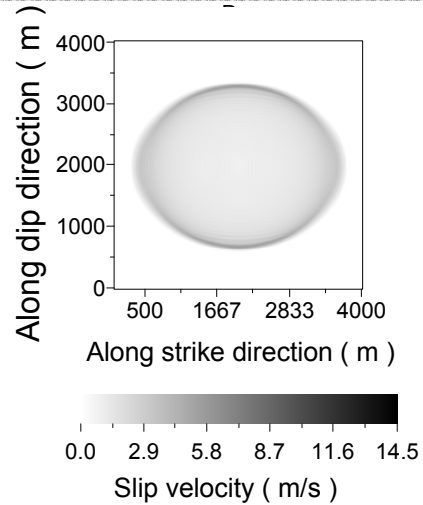
$$\begin{aligned} \tilde{p}_{fluid}^{wf}(\xi_1, \xi_3, t) = & p_{fluid_0}^f + \frac{\gamma}{2w(\xi_1, \xi_3)} \int_0^{t-\varepsilon} dt' \left\{ -\frac{\chi}{\omega - \chi} \operatorname{erf}\left(\frac{w(\xi_1, \xi_3)}{2\sqrt{\chi(t-t')}}\right) + \frac{\omega}{\omega - \chi} \operatorname{erf}\left(\frac{w(\xi_1, \xi_3)}{2\sqrt{\omega(t-t')}}\right) \right\} \\ & \left\{ \tau(\xi_1, \xi_3, t') v(\xi_1, \xi_3, t') - \frac{2w(\xi_1, \xi_3)}{\gamma} \frac{1}{\beta_{fluid} \Phi(t')} \frac{\partial}{\partial t'} \Phi(\xi_1, 0, \xi_3, t') \right\} \end{aligned}$$



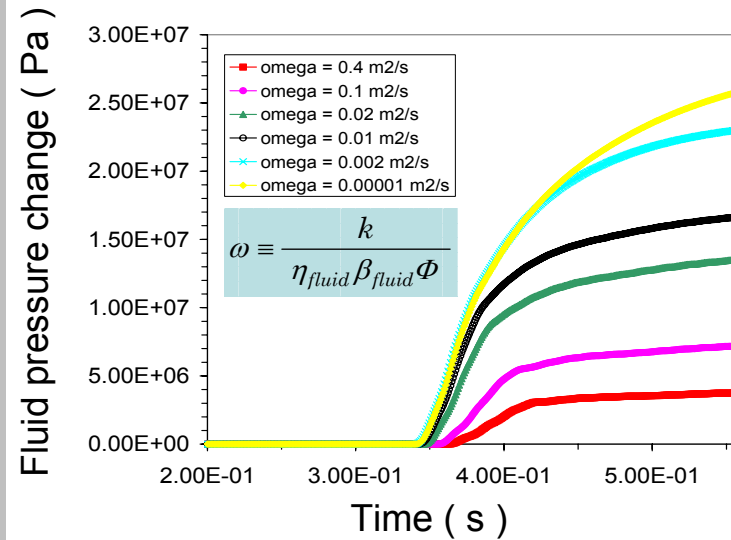
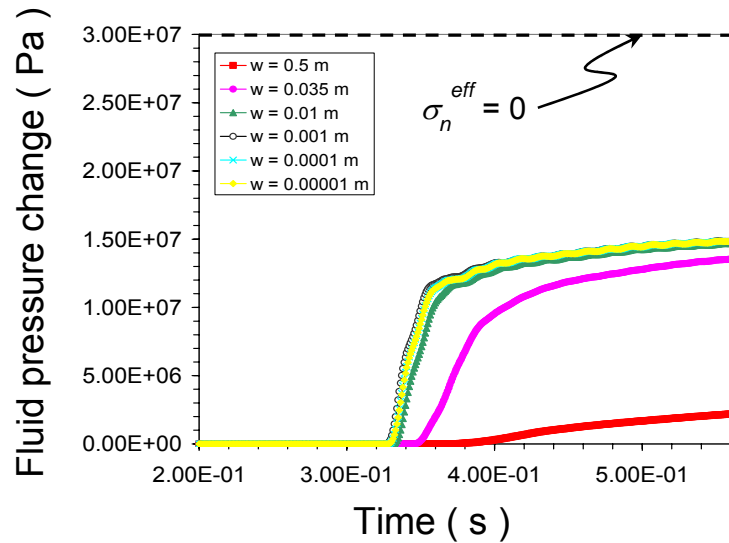
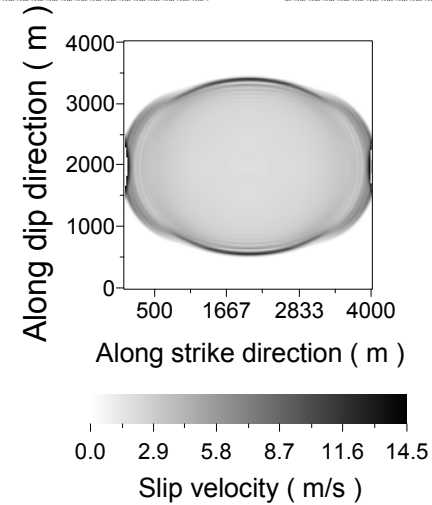
# Results with SW law



## Dry fault ( $\sigma_n^{eff} = \text{const}$ )

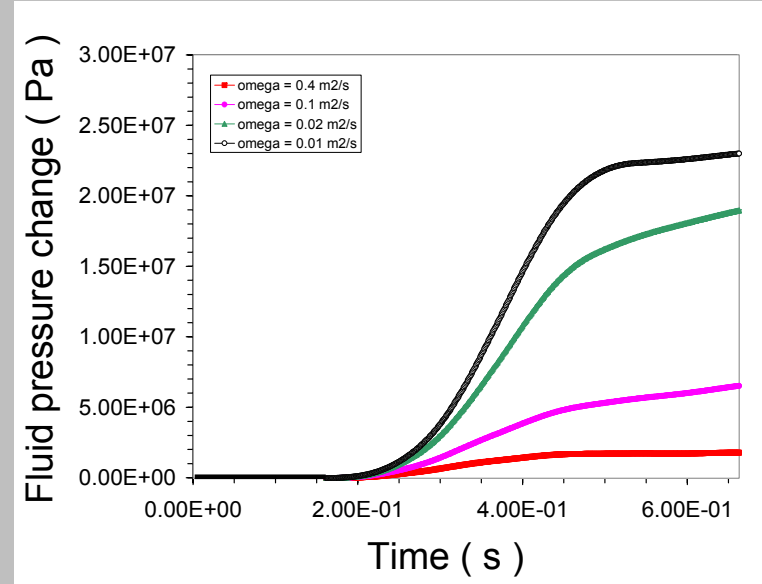
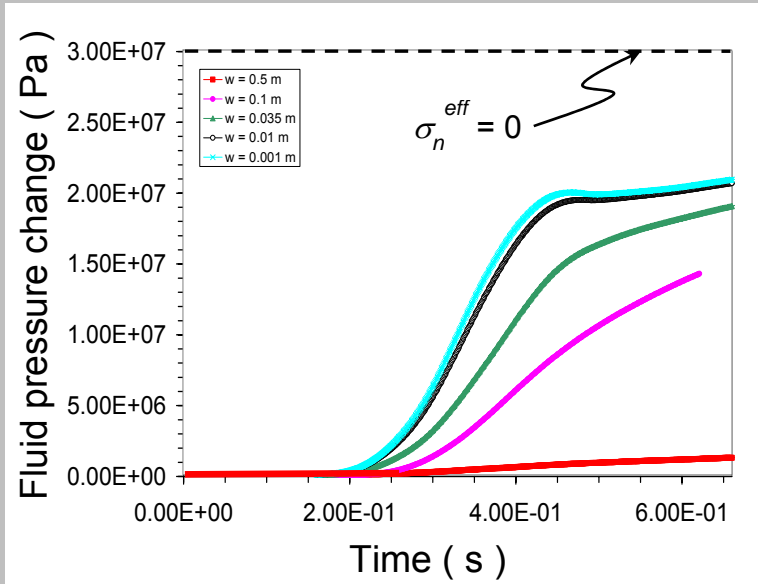


## Wet fault ( $\sigma_n^{eff}$ varies )



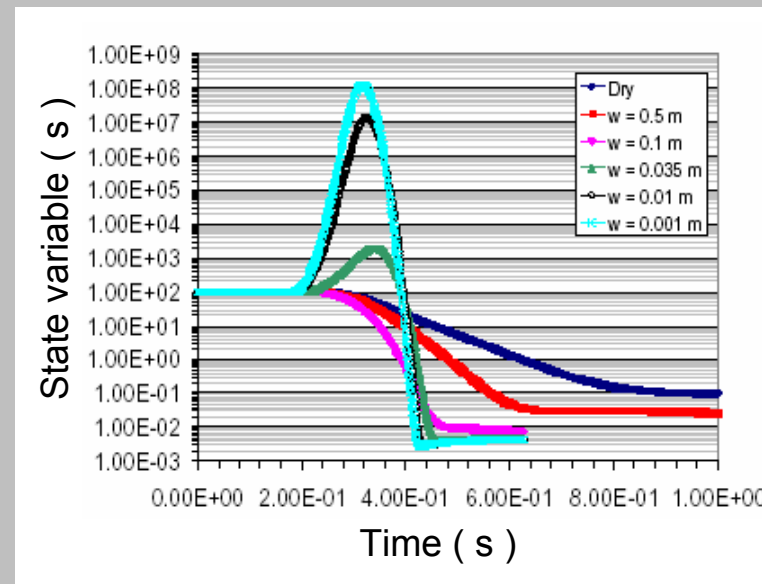
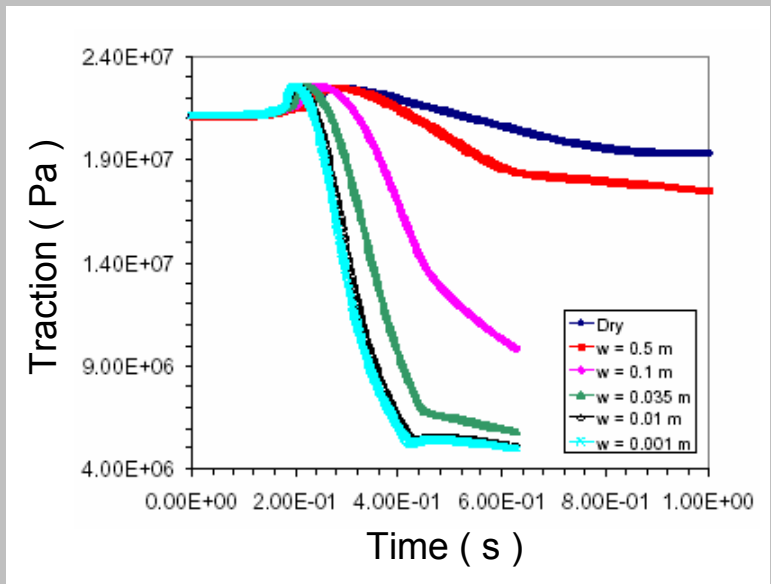
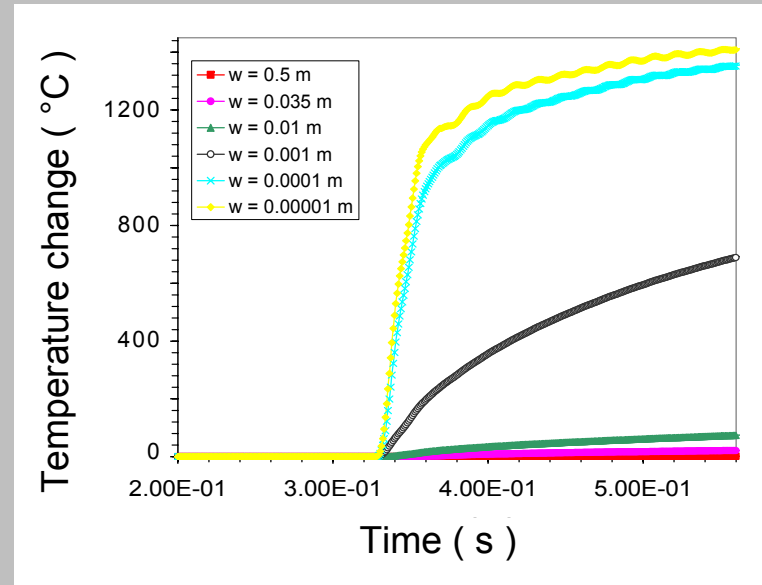
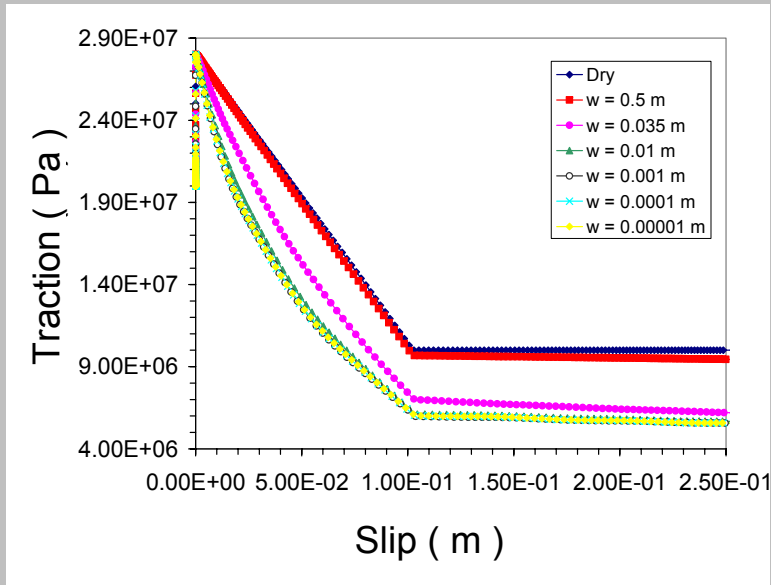


# Results with DR law





# The breakdown zone



An aerial photograph of a vast, flat, and wet landscape, likely a coastal plain or a large field after heavy rain. The ground is a mix of dark, saturated mud and lighter, wet sand, with numerous small puddles and channels of water scattered across the surface. The overall tone is greyish-brown. In the center of the image, there is a semi-transparent grey rectangular box containing text.

**II. Flash heating  
of micro – asperity contacts**

# Mathematical background

## RUINA – DIETERICH WITH FLASH HEATING

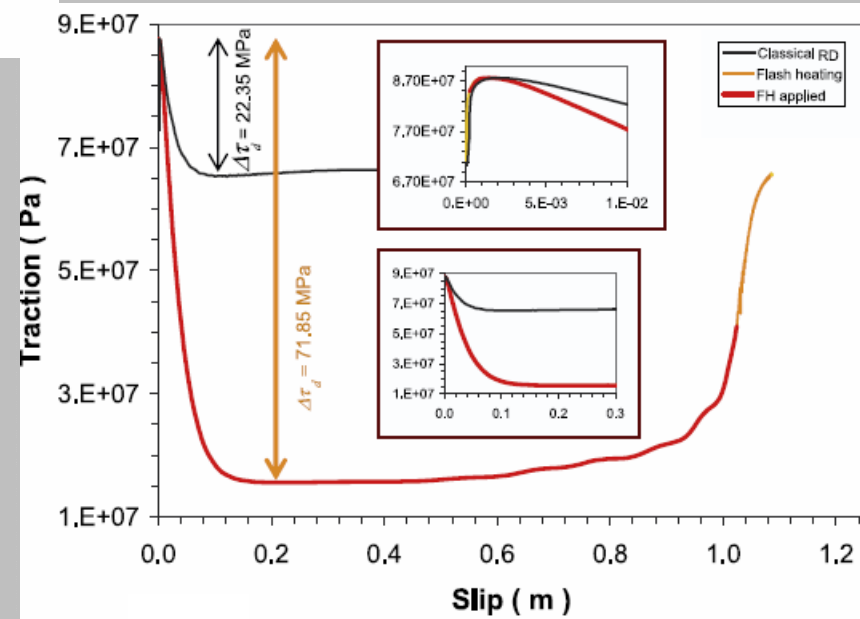
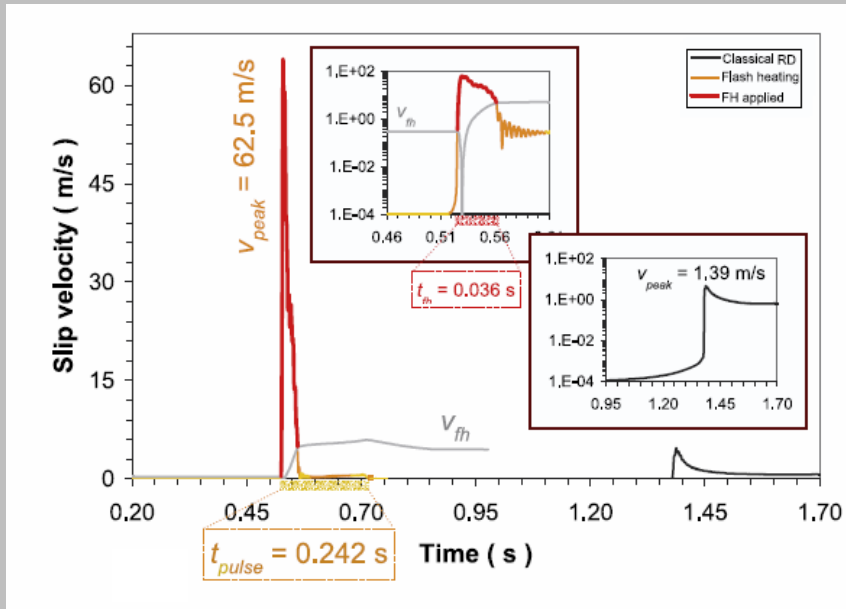
$$\left\{ \begin{array}{l} \tau = \left[ \mu_* - a \ln\left(\frac{v_*}{v}\right) + \theta \right] \sigma_n^{eff} \\ \frac{d}{dt} \theta = \begin{cases} -\frac{v}{L} \left[ \theta + b \ln\left(\frac{v}{v_*}\right) \right] & , v \leq v_{fh} \\ -\frac{v}{L} \left[ \theta + b \frac{v_{fh}}{v} \ln\left(\frac{v}{v_*}\right) + \left(1 - \frac{v_{fh}}{v}\right) \left( a \ln\left(\frac{v}{v_*}\right) + \mu_* - \mu_{fh} \right) \right] & , v > v_{fh} \end{cases} \end{array} \right.$$

where  $v_{fh} = \frac{\pi\chi}{D_{ac}} \left( c \frac{T_{weak} - T^{wf}}{\tau_{ac}} \right)^2$  is

a weakening velocity above which flash heating is activated,  $T_{weak}$  is a weakening temperature,  $\tau_{ac}$  is the ( average ) shear strength of asperity contacts and  $D_{ac}$  their ( average ) size.



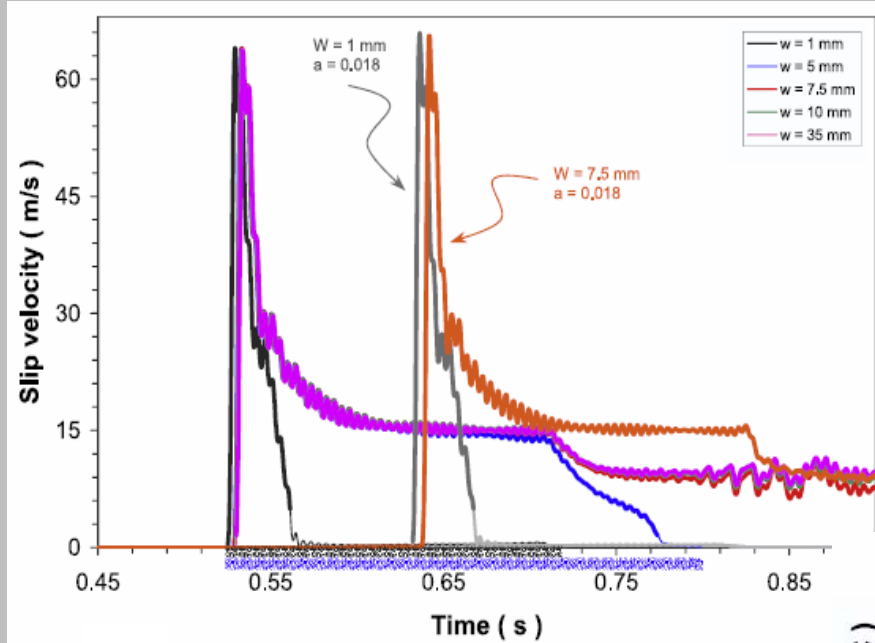
# Crack - like ruptures or slip pulses?



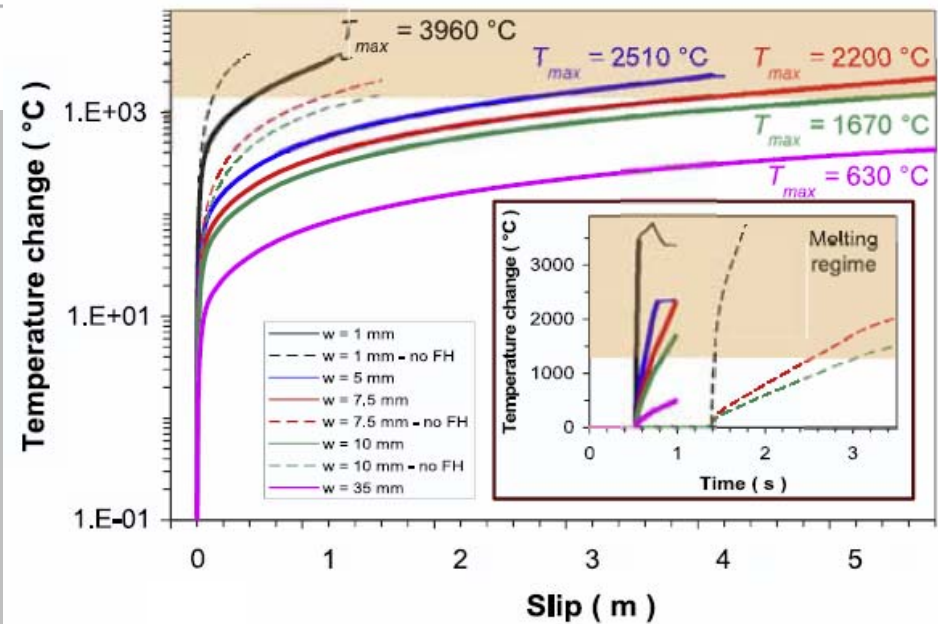




# The prominent importance of $2w$



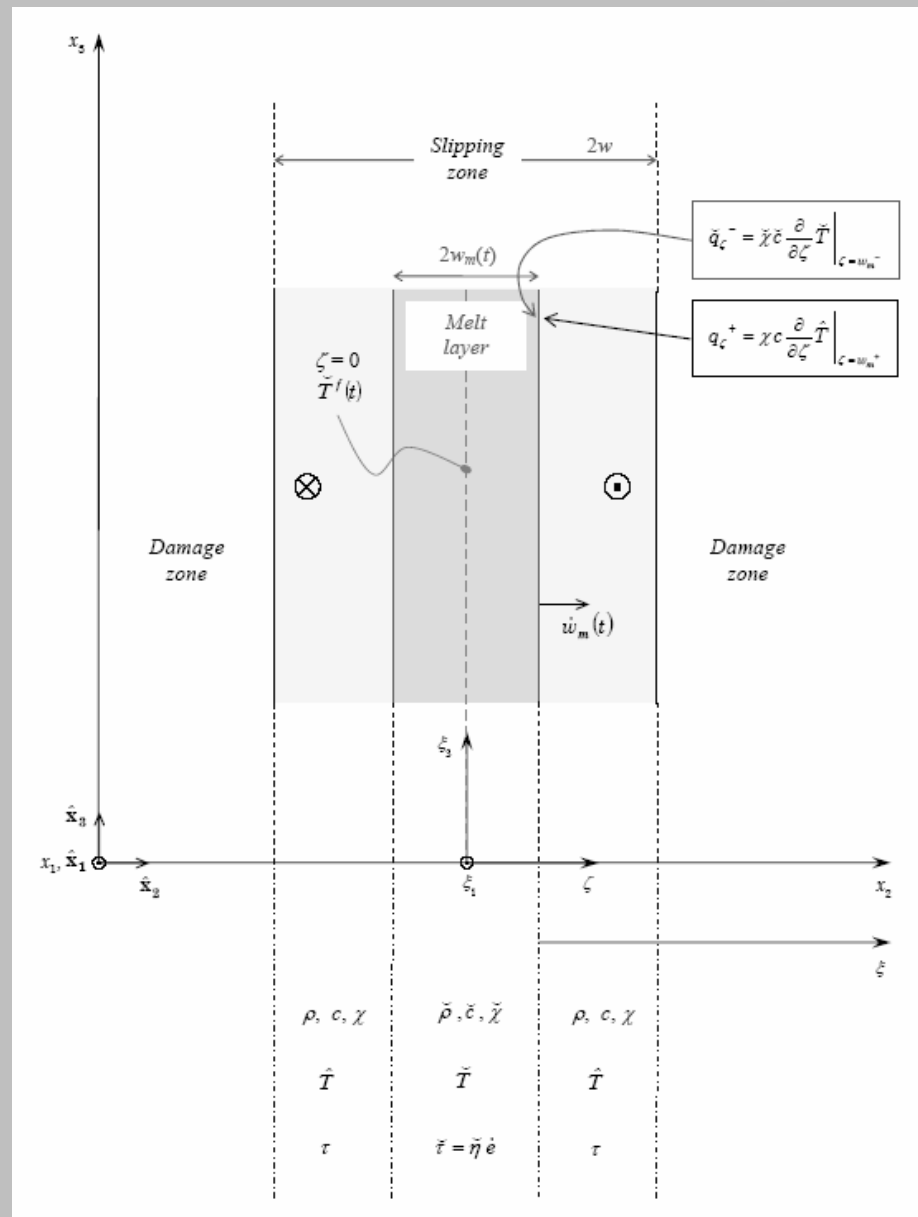
Localized shear ( $2w \leq 10 \text{ mm}$ ):  
self-healing pulses



An aerial photograph showing a complex network of meltwater channels and ponds on a light-colored, possibly glacial, terrain. The water is a mix of white, grey, and brownish colors, indicating varying depths and sediment content. The channels are irregular and interconnected, creating a maze-like pattern across the landscape. A semi-transparent grey rectangular box is centered over the image, containing the text 'III. Melting of rocks and gouge' in a bold, red, sans-serif font.

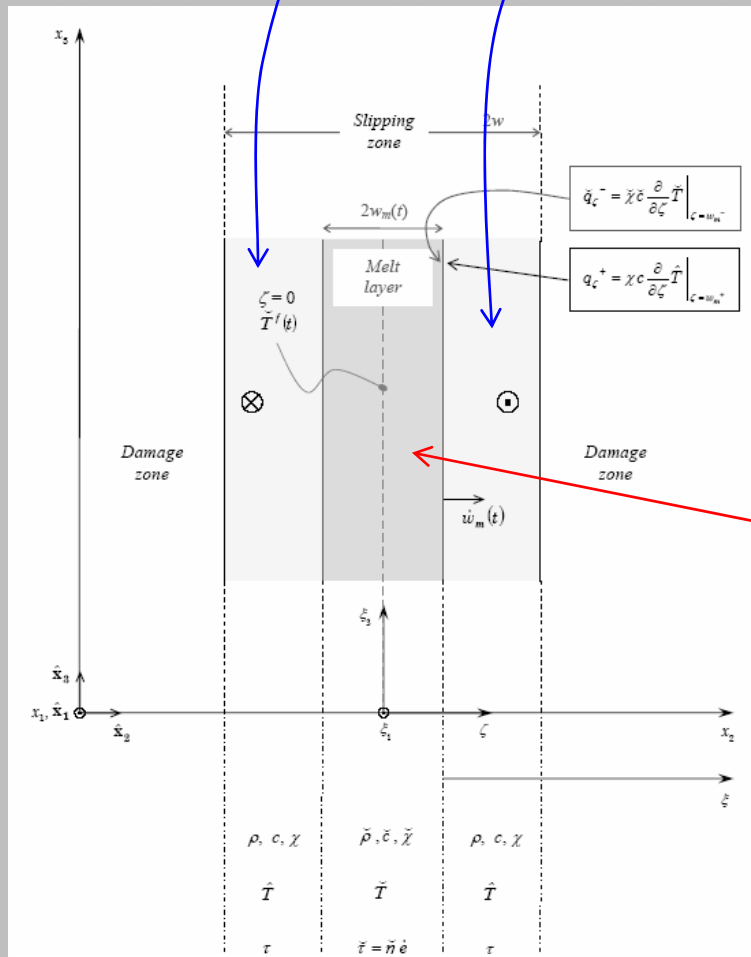
### **III. Melting of rocks and gouge**

# Mathematical background



Bizzarri (2010, JGR)

# Mathematical background



Bizzarri (2010, JGR)

$$\frac{\partial}{\partial t} T(\zeta, t) = \chi \frac{\partial^2}{\partial \zeta^2} T(\zeta, t) + \frac{1}{c} q(\zeta, t)$$

$$q(\zeta, t) = \begin{cases} \frac{\tau(t)v(t)}{2w} & , t > 0, |\zeta| \leq w \\ 0 & , |\zeta| > w \end{cases}$$

$$T^f(t) \equiv T(0, t) = T_0^f + \frac{1}{2cw} \int_0^{t-\varepsilon} dt' \operatorname{erf} \left( \frac{w}{2\sqrt{\chi(t-t')}} \right) \tau(t')v(t')$$

$$\frac{\partial}{\partial t} \tilde{T}(\zeta, t) = \tilde{\chi} \frac{\partial^2}{\partial \zeta^2} \tilde{T}(\zeta, t) + \frac{d}{dt} w_m(t) \frac{\partial}{\partial \zeta} \tilde{T}(\zeta, t) + \frac{1}{c} \tilde{q}(\zeta, t)$$

$$\tilde{q}(\zeta, t) = \frac{\tilde{\tau}(\zeta, t) v(t) e^{-\frac{\zeta^2}{2w_m^2(t)}}}{\sqrt{2\pi} w_m(t)} \Theta(t - t_m)$$

$$\tilde{T}^f(t) \equiv \tilde{T}(0, t) = T_m + \frac{\left( \sqrt{\frac{2\pi}{e}} + \pi \operatorname{erf} \left( \frac{1}{\sqrt{2}} \right) - \sqrt{2\pi} \right)}{2\pi \tilde{c} \tilde{\chi}} \cdot \Theta(t - t_m) w_m(t) \tilde{\tau}(t)v(t).$$

# Mathematical background

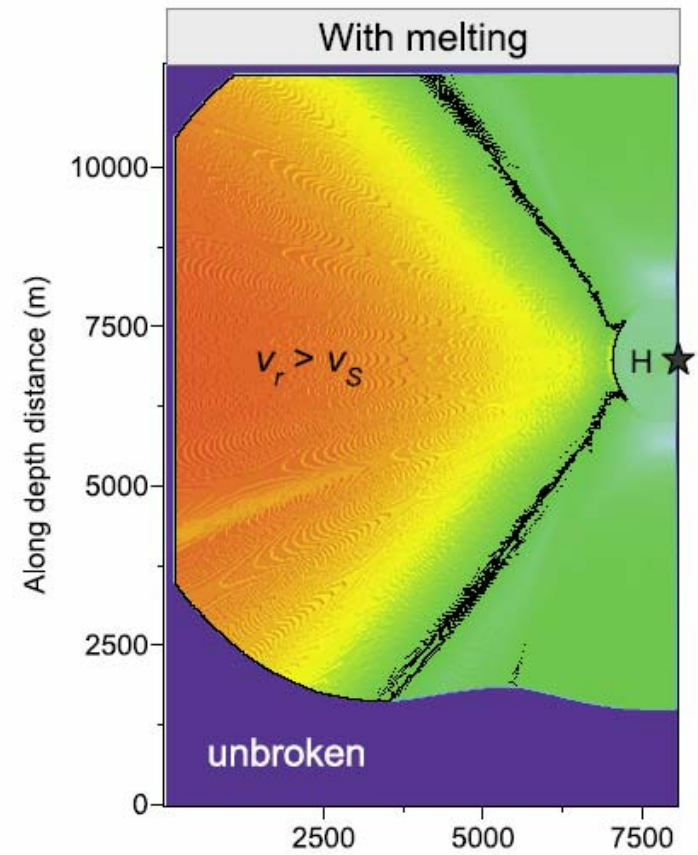
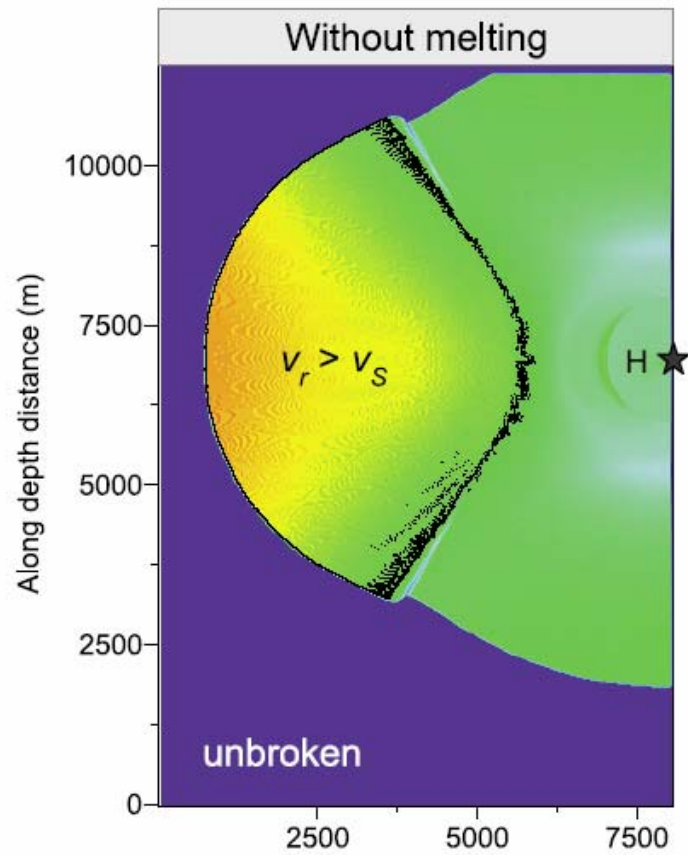
Coulomb friction is no longer valid and we then consider a Newtonian fluid (e.g., Fialko, 2004):

$$\tau^{(\text{NF})} = \tilde{\eta} \frac{v}{2w_m}$$

$$\tilde{\eta}(\zeta, t) = \tilde{K} e^{\frac{\tilde{T}_a}{T(\zeta, t - \varepsilon) + 273.15}}$$

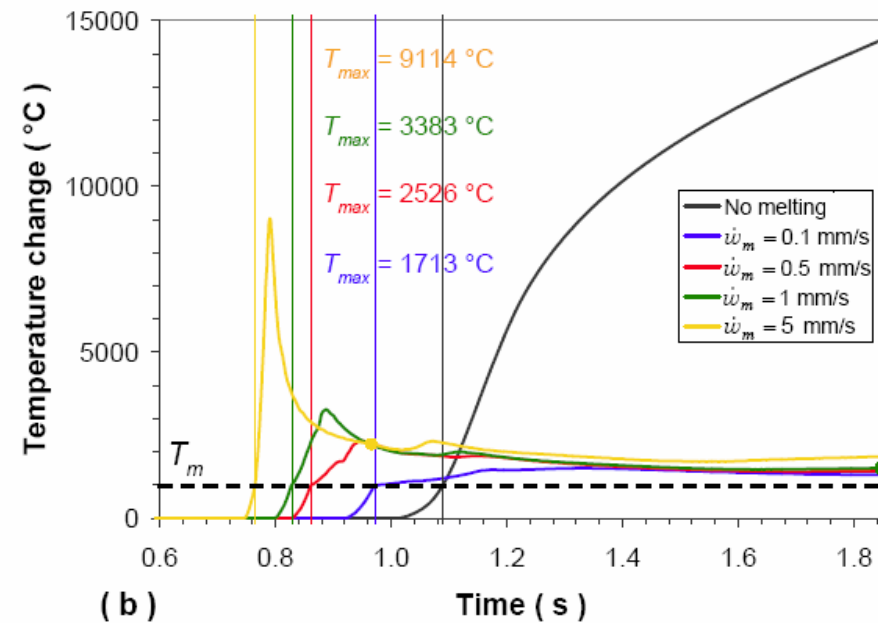
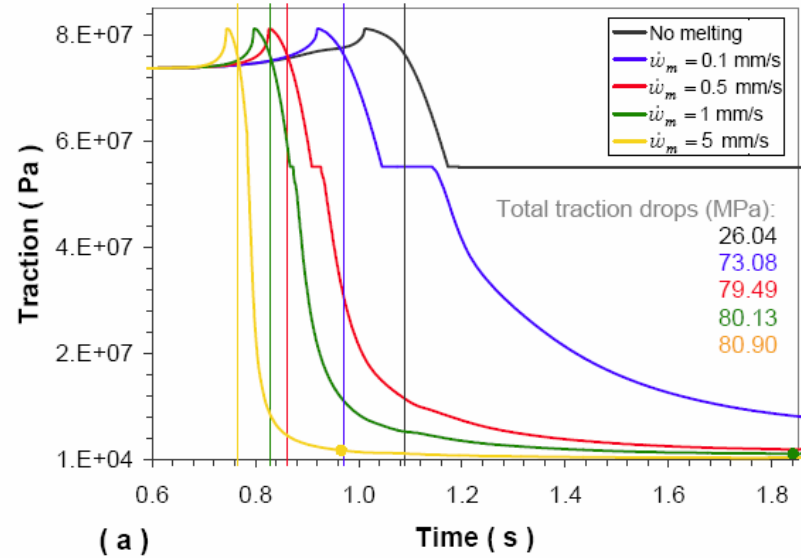
3-D

# Melting enhances supershear EQs





# Transition to a viscous rheology



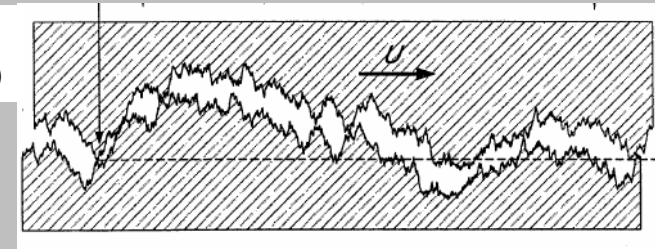
An aerial photograph of a coastal wetland or marsh. The landscape is a mix of dark, water-saturated mudflats and lighter, sandy or silty areas. There are several small, irregular pools of water scattered throughout. The overall appearance is that of a natural, undisturbed coastal environment. A semi-transparent grey rectangular box is centered over the image, containing the text 'IV. Mechanical lubrication' in a bold, red, sans-serif font.

## **IV. Mechanical lubrication**



# Mathematical background

Brodsky and Kanamori (2001)



$$\tau = \begin{cases} \mu_u \sigma_n^{\text{eff}} + \frac{\langle 2w \rangle}{u} p_{\text{lub}} = \mu_u \sigma_{n_0} - \left( \mu_u - \frac{\langle 2w \rangle}{u} \right) p_{\text{lub}} & , So < 1 \\ \frac{\langle 2w \rangle}{u} p_{\text{lub}} & , So \geq 1 \end{cases}$$

Effective normal stress  $\sigma_n^{\text{eff}} = \sigma_n - p_{\text{res}} - p_{\text{lub}}$

Sommerfeld number  $So \equiv \frac{p_{\text{res}} + p_{\text{lub}}}{\sigma_n}$

$$\langle 2w \rangle^3 p_{\text{lub}} - 6\eta r u^2 v = 0$$

In the special case of (temporally) constant gap height ( $\langle 2w \rangle = \langle 2w_0 \rangle$ )

Lubrication pressure

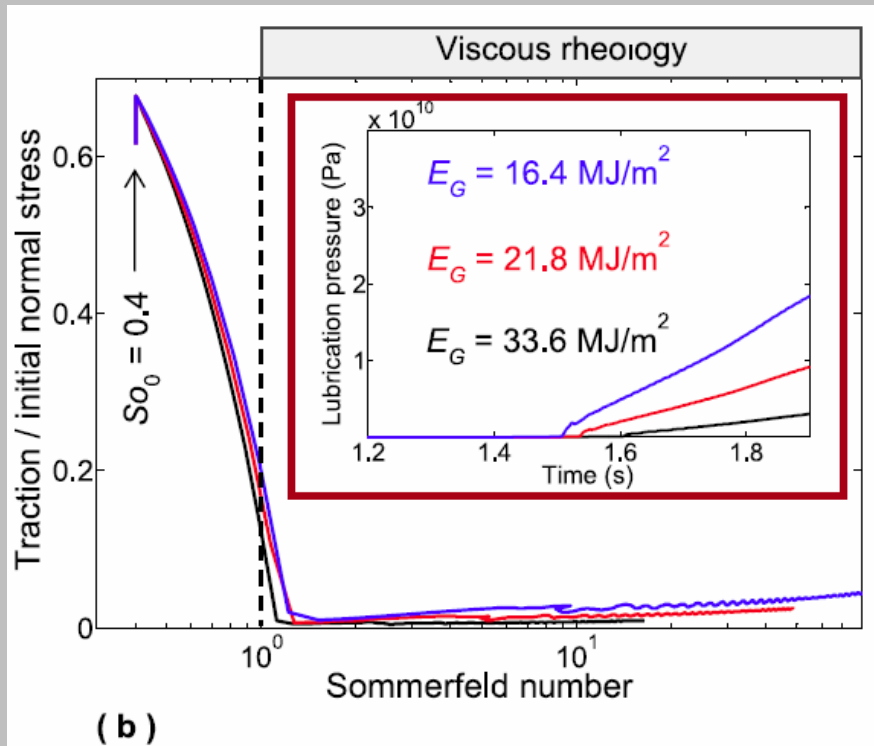
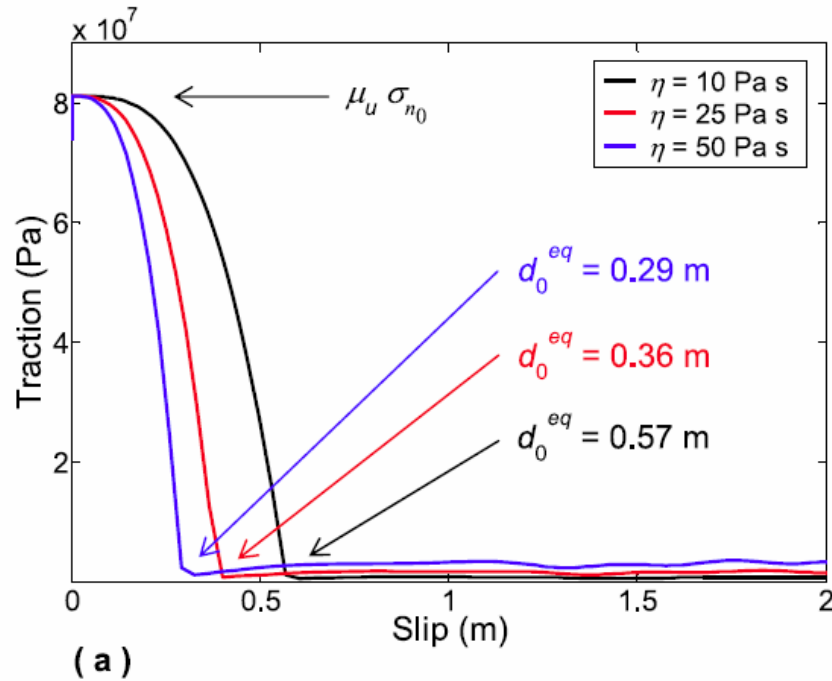
Frictional resistance

$$\begin{cases} \frac{6\eta r}{\langle 2w_0 \rangle^3} u^2 v \\ \left\{ \begin{array}{l} \mu_u \sigma_{n_0} - \frac{6\eta r \mu_u}{\langle 2w_0 \rangle^3} u^2 v + \frac{6\eta r}{\langle 2w_0 \rangle^2} u v & , So < 1 \\ \frac{6\eta r}{\langle 2w_0 \rangle^2} u v & , So \geq 1 \end{array} \right. \end{cases}$$

Bizzarri (2012, *JGR*, **117**, B05304)



# Viscous rheology after $So = 1$



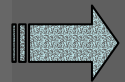
# Conclusions

- ✓ Many different physical and chemical mechanisms may occur during faulting
- ✓ They strongly affect the overall dynamics of the fault, the radiated energy and the resulting ground motions
- ✓ Thermal pressurization of pore fluids, flash heating, melting and mechanical lubrication tend to enhance supershear ruptures...
- ✓ ... produce a nearly complete stress drop ( heat paradox )
- ✓ ... increase the ( equivalent ) slip–weakening distance and thus the “fracture” energy
- ✓ In some cases the weakening behavior becomes exponential, as suggested by laboratory observations

- ✓ Different competing mechanisms can significantly affect the recurrence time of an earthquake sequence...
- ✓ ... and they can make the concept itself of the seismic cycle meaningless

# Open questions and future developments

- 1) Theoretical results will predict a nearly complete stress drop and therefore we should find a signature of these high stress drop values in the recorded seismograms. Seismological estimates of stress drop do not support such an evidence;



the estimation of stress drop from seismic waves is biased ( for instance by the difficulties in analyzing high frequency radiation )

or

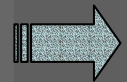
the effects of pressurization, melting and so on on the dynamic traction evolution are less pronounced

2) We need to test theoretical predictions against laboratory evidence; numerical results definitively represent an input for the development of next-generation machines

⇒ Current high velocity lab. experiments only deal with friction ( of pre-cut surfaces ) and not with fracture ( of intact rocks )

⇒ We need to reproduce real-world conditions in terms of BOTH high sliding velocity and confining stress

3) Do real data (recorded during natural earthquakes) contain signatures of the specific friction law governing the sesimogenic fault?



We know from numerical models that, for ruptures having exactly the same energetics ( namely, the same fracture energy density ), the resulting ground motions are virtually indistinguishable

# A multidisciplinary approach

## ***Theoretical models***

of the fault constitutive behavior based on rock physics

## ***Numerical models***

of the fault response, given some hypotheses on the fault geometry, governing eqts., initial conditions, ...

## ***Inferences from data***

recorded during a real event and analysis of some specific signatures of the rupture dynamics (e.g., kinematic inversions, spectral analysis of ground motions, etc.)

## ***Geological observations***

conducted in the field (exhumed faults) and by analyzing samples in the laboratory

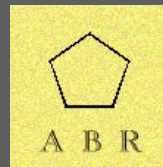
## ***Laboratory experiments***

conducted in “realistic” conditions on rock (or gouge) samples



**Thank you!**

**This slide is empty intentionally.**



# **Support Slides: Parameters, Notes, etc.**

*To not be displayed directly. Referenced above.*

# Why “ *truly* “ 3 – D ?



2 – D Mode II ( pure in – plane ):  $\mathbf{u} = (u_1(x_1, t), 0, 0)$

2 – D Mode III ( pure anti – plane ):  $\mathbf{u} = (0, u_2(x_1, t), 0)$

3 – D Mixed mode:  $\mathbf{u} = (u_1(x_1, t), u_2(x_1, t), 0)$

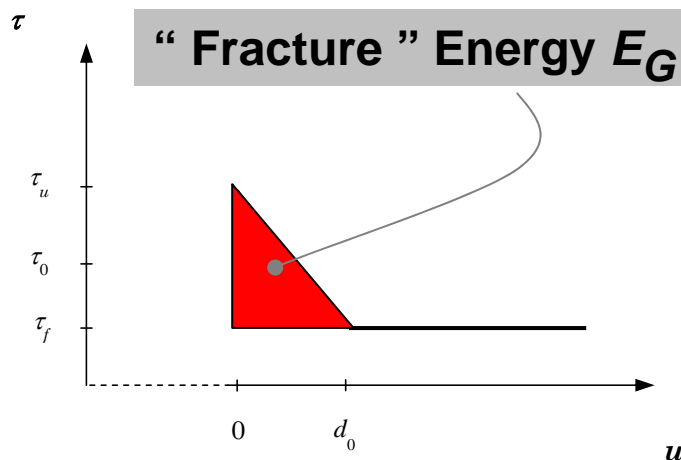
3 – D having only one non null component:  $\mathbf{u} = (u_1(x_1, x_2, t), 0, 0)$

*Truly* 3 – D:  $\mathbf{u} = (u_1(x_1, x_2, t), u_2(x_1, x_2, t), 0)$

# Slip - Weakening Friction Laws



$$\tau = \begin{cases} \left[ \mu_u - (\mu_u - \mu_f) \frac{u}{d_0} \right] \sigma_n^{eff} & , u < d_0 \\ \mu_f \sigma_n^{eff} & , u \geq d_0 \end{cases}$$



Barenblatt ( 1959a, 1959b ), Ida ( 1972 ), Andrews ( 1976a, 1976b ), and many authors thereafter

$d_0$  is the characteristic slip – weakening distance

# Rate - and State - Dependent

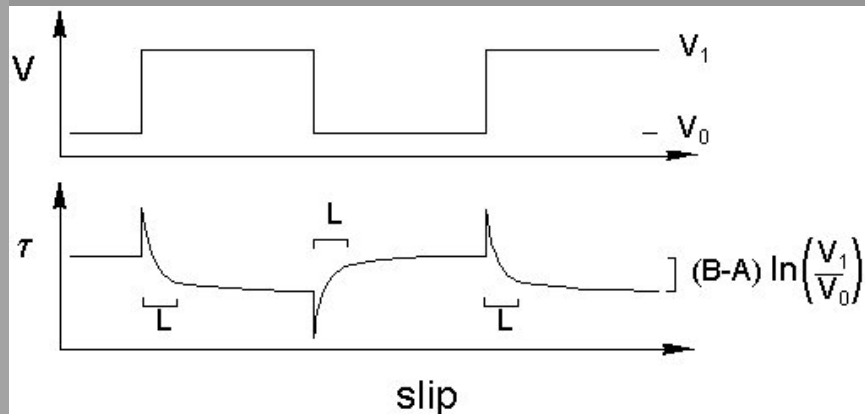


## DIETERICH – RUINA WITH VARYING NORMAL STR.

$$\left\{ \begin{array}{l} \tau = \left[ \mu_* - \alpha \ln \left( \frac{v_*}{v} \right) + b \ln \left( \frac{\Psi v_*}{L} \right) \right] \sigma_n^{eff} \\ \frac{d}{dt} \Psi = 1 - \frac{\Psi v}{L} - \left( \frac{\alpha_{LD} \Psi}{b \sigma_n^{eff}} \right) \frac{d}{dt} \sigma_n^{eff} \end{array} \right.$$

*Linker and Dieterich ( 1992 ), Dieterich and Linker ( 1992), Bizzarri and Cocco ( 2006a, 2006b )*

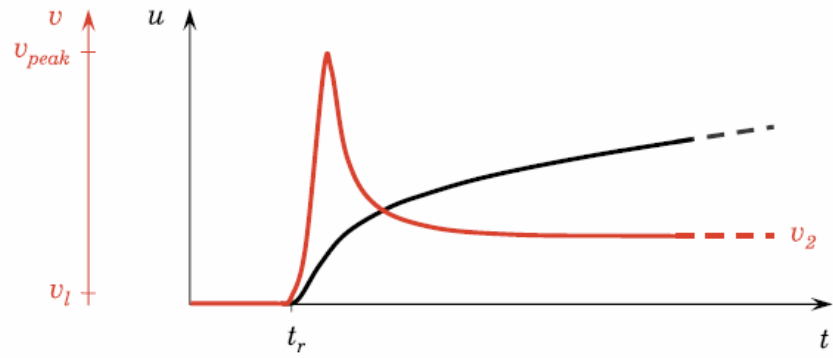
### Response to an abrupt jump in load



# Crack vs. Pulse

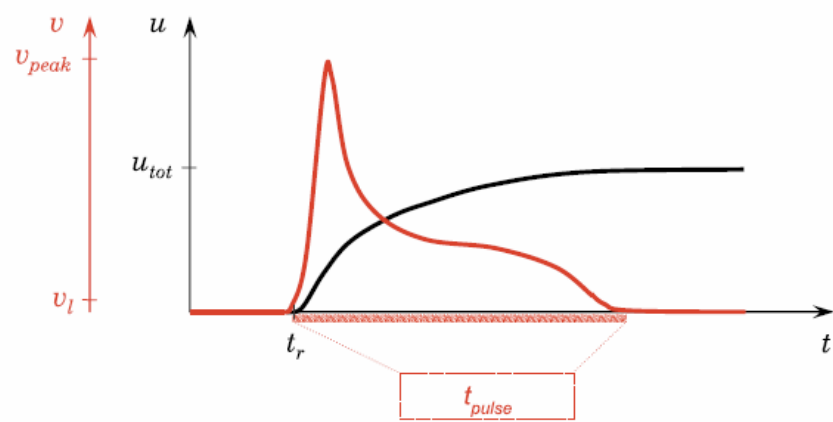


Crack-like rupture



(a)

Pulse-like rupture



(b)